Symmetric solutions of the n-body problem: A numerical study of Floquet multipliers and Morse indices

Astronomy and Computing 55 (2026) 101085

Contents lists available at ScienceDirect

Astronomy and Computing

journal homepage: www.elsevier.com/locate/ascom

Full length paper

Symmetric solutions of the n-body problem: A numerical study of Floquet multipliers and Morse indices☆

Diego Berti [a], Gian Marco Canneori [a], Roberto Ciccarelli [a], Irene De Blasi [a,*], Margaux Introna [b,a], Davide Polimeni [a]

[a] Department of Mathematics, University of Turin, Via Carlo Alberto 10, Turin, 10123, Italy
[b] Department of Physics, University of Trento, Via Sommarive 14, Povo, TN, 38123, Italy

ARTICLE INFO

Keywords:
N-body problem
Symmetric periodic orbits
Floquet multipliers
Morse index

ABSTRACT

In this paper, we consider periodic solutions of the n-body problem that satisfy symmetry constraints, expressed through invariance under finite group actions. We focus on their stability properties and present algorithms specifically designed for the computation of Floquet multipliers and Morse indices. Numerical results are provided to illustrate our methods in both two and three dimensional configuration spaces, and for different choices on the number of bodies.

1. Introduction

The n-body problem stands as one of the most important and challenging models in celestial mechanics, having attracted the attention of mathematicians and physicists for centuries. Its formulation is both clear and simple: consider n massive particles in the space, subject to their mutual gravitational attraction, in the framework of classical mechanics.[1] Starting from given initial conditions, the question is whether one can understand and predict the qualitative behaviour of their motion. Gravitational Newton laws provide the motion equations of $x_1, \dots, x_n \in \mathbb{R}^3$ heavy bodies with masses $m_1, \dots, m_n > 0$, which read

$$m_k \ddot{x}_k(t) = -\sum_{j \neq k} m_k m_j \frac{x_k(t) - x_j(t)}{\|x_k(t) - x_j(t)\|^3}, \quad \text{for each } k \in \{1, \dots, n\},$$

where $\|\cdot\|$ is the Euclidean norm of $\mathbb{R}^3$. As a first observation, any collision between two or more bodies is a singularity of the motion equations and breaks the completeness of the associated flow.

As a matter of fact, what appears to be an elementary formulation soon reveals a remarkable complexity as the number of bodies increases. When only 2 bodies are involved, we deal with the famous *Kepler problem*, which is an example of completely integrable system (i.e., starting from any initial configuration, closed formulæ for solutions can be found). The regular property of integrability is broken by introducing one or more additional bodies in the picture, as remarkably noticed in the pioneering studies of Poincaré (1893). Small changes in the initial conditions of known solutions can lead to unexpected and unpredictable phenomena, raising a reasonable conjecture on the deterministic chaos of the n-body problem (see Moser, 1973; Bolotin, 2006; Llibre and Simó, 1980; Guardia et al., 2016; Boekholt et al., 2020; Leigh et al., 2016). Moreover, interesting open questions on the long term behaviour and qualitative description of such systems still persist (see the book Montgomery, 2024).

Henri Poincaré conjectured that periodic orbits are dense in the 3-body problem and claimed that they play a central role in capturing the system's complexity. In this picture, periodic orbits provide a systematic and useful tool to approximate increasingly intricate trajectories, serving as empirical validation of topological chaos. For this reason, the community has shown great interest in finding periodic solutions for the n-body problem, employing both numerical and analytical approaches. In particular, since the 90s, variational methods have been successfully applied to produce collision-free periodic solutions (see Bahri and Rabinowitz, 1991; Serra and Terracini, 1992; Majer and Terracini, 1993a,b, 1995). In short, one can consider the Lagrange action functional associated with the motion equations

$$\mathcal{A}(x) = \int_0^T \left[\frac{1}{2} \sum_{i=1}^n m_i \|\dot{x}_i(t)\|^2 + \sum_{i<j} \frac{m_i m_j}{\|x_i(t) - x_j(t)\|} \right] dt$$

and look for its critical points, which naturally correspond to solutions of the n-body problem through a least action principle. Among all

☆ This article is part of a Special issue entitled: 'HPC in Cosmology and Astrophysics' published in Astronomy and Computing.

* Corresponding author.
E-mail address: irene.deblasi@unito.it (I. De Blasi).

[1] We highlight that a relativistic study might be possible (see Di Ruzza, 2021), but the application of the hereby presented methods to such case lie outside the aim of this paper.

https://doi.org/10.1016/j.ascom.2026.101085
Received 28 October 2025; Received in revised form 18 January 2026; Accepted 17 February 2026
Available online 17 February 2026

periodic solutions, one can focus on those who satisfy a symmetry constraint, especially if this restriction makes the search of critical points more feasible. The first successful effort for the planar n-body problem traces back to Bessi and Zelati (1991), where the authors proved the existence of non-collision solutions using variational methods. Later on, in the celebrated paper (Chenciner and Montgomery, 2000), Alain Chenciner and Richard Montgomery proved the existence of the spectacular figure-eight solution, previously discovered in Moore (1993). Subsequently, Davide Ferrario and Susanna Terracini enlarged the range of applicability of variational methods to symmetric n-body problems in the celebrated paper (Ferrario and Terracini, 2004). Discovering elementary algebraic conditions, they allow to consider a wide class of symmetries, in which periodic solutions can be found. The symmetry constraint on the configurations of the bodies is expressed by using the action of a finite group G, and they look for critical points of the action functional among G-equivariant loops. Notably, variational methods produced many other results in the last two decades, enlarging the set of symmetric periodic solutions for the n-body problem (see, e.g., Chen, 2001; Ramos and Terracini, 1995; Chenciner and Venturelli, 2000; Barutello and Terracini, 2004; Fusco et al., 2011; Simó, 2001b).

Back to the paper Ferrario and Terracini (2004), alongside with a huge theoretical effort to deal with collisions between the bodies and to provide a solid theory on G-equivariant loops, the authors conceived a useful algorithm to produce numerical symmetric solutions. Their theoretical results found a practical confirmation and the software *symorb* was created (dlfer, 2017; Ferrario, 2024). It consists of a numerical pipeline based on a combination of Python, Fortran and GAP, which allows to choose a finite group, consider the symmetry involved and look for equivariant critical points of the action functional.

Recently, a new version of the original software was presented in DipMathUniTO (2024), Barutello et al. (2026). Distributed as a Julia package, *SymOrb.jl* represents a profound and modular redesign of the previous implementation. This new architecture provides a flexible and extensible framework, enabling seamless integration of both quantitative and qualitative tools, such as stability analysis and topological index computations. It also introduces more efficient optimisation routines, improving computational performance. Finally, the new structure of *SymOrb.jl* enables the systematic organisation of symmetric orbits into databases and supports advanced numerical methods.

Starting from a collection of numerical results produced with *SymOrb.jl*, the present paper aims to establish a set of benchmark cases, by examining their stability properties under variations of the action and small perturbations of the orbits' initial conditions. To this end, two classical stability indicators are considered: the Morse index and the Floquet multipliers (Morse, 1934; Smale, 1965; Teschl, 2012). We also outline the main steps required to compute a numerical approximation of these indicators in our setting.

Overall, this work offers a first comprehensive illustration of how *SymOrb.jl*, complemented by its stability modules, can be employed to find highly accurate numerical approximations of solutions to the n-body problem and to analyse their stability through different methodological approaches.

Mathematical setting and problem statement. For $n \geq 2$ particles, we denote their masses as $m_1, \dots, m_n > 0$ and their positions as $x_i \in \mathbb{R}^d$, where $d = 2, 3$. Since the n-body problem is a mechanical system, we can introduce the potential function

$$U(x_1, \dots, x_n) = \sum_{j<i} \frac{m_j m_i}{\|x_j - x_i\|}, \quad \|\cdot\| \text{ Euclidean norm of } \mathbb{R}^d,$$

so that the equation of motion of the $i-$th particle is given by

$$m_i \ddot{x}_i(t) = \frac{\partial U}{\partial x_i}(x_1(t), \dots, x_n(t)). \tag{1}$$

It is easy to see that the centre of mass of the system is invariant under translations, so it is useful to fix it at the origin and to introduce the configuration space

$$\mathcal{X} := \left\{ x = (x_1, \dots, x_n) \in (\mathbb{R}^d)^n \ : \ \sum_{i=1}^n m_i x_i = 0 \right\}.$$

Note that the potential function U has a singularity whenever $x_i = x_j$ for some $j \neq i$. The singularity set of U can be described as follows

$$\Delta_{ij} = \left\{ x \in \mathcal{X} \ : \ x_i = x_j \right\}, \quad \Delta = \bigcup_{i,j} \Delta_{ij},$$

and, as a consequence, the set of non-colliding configurations is nothing but $\hat{\mathcal{X}} = \mathcal{X} \setminus \Delta$. We also define the kinetic energy as

$$K(\dot{x}) = \frac{1}{2} \sum_{i=1}^n m_i \|\dot{x}_i\|, \quad \dot{x} = (\dot{x}_1, \dots, \dot{x}_n) \in T_x \mathcal{X},$$

where $T_x\mathcal{X}$ denotes the tangent space to $\mathcal{X}$ at $x \in \mathcal{X}$. In this way, the Lagrangian function associated to Eqs. (1) can be expressed as

$$L(x, \dot{x}) = U(x) + K(\dot{x}).$$

Classical periodic solutions of (1) are trajectories $x(t) = (x_1(t), \dots, x_n(t)) \in \hat{\mathcal{X}}$ such that $x(T) = x(0)$ for a suitable $T > 0$: the smallest T that satisfies this condition is called the *period* of the orbit. Given $T > 0$, let us then define the torus of length T as $\mathbb{T} = \mathbb{R}/T\mathbb{Z}$, and consider the space of H^1 *T-periodic loops* (possibly with collisions between the bodies)

$$\Lambda = H^1(\mathbb{T}; \mathcal{X}) = \left\{ x, \dot{x} \in L^2([0, T], \mathcal{X}) \ : \ x(0) = x(T) \right\}.$$

We then denote by

$$\hat{\Lambda} = H^1(\mathbb{T}; \hat{\mathcal{X}}) \subset \Lambda$$

the open sub-set of collision-less loops. The Lagrange action functional on Λ reads

$$\begin{aligned} \mathcal{A}(x) &= \int_0^T L(x(t), \dot{x}(t))\, dt \\ &= \int_0^T \left[\frac{1}{2} \sum_{i=1}^n m_i \|\dot{x}_i(t)\|^2 + \sum_{i<j} \frac{m_i m_j}{\|x_i(t) - x_j(t)\|} \right] dt \end{aligned} \tag{2}$$

and has the following property: if $x \in \hat{\Lambda}$ is a critical point of $\mathcal{A}$, then x is a T-periodic solution of (1) (see Ferrario and Terracini, 2004). This is the variational principle we are going to refer to in order to find $T-$periodic solutions of our system.

Group actions, G-equivariance and optimisation. In this paragraph we briefly recall the basic definitions needed to impose symmetry constraints in the bodies motions. Our main reference here is Ferrario and Terracini (2004), while the interested reader can find a detailed account on G-equivariance and group actions in Barutello et al. (2026).

Let G be a finite group; we say that G acts on a set X if there exists a map $\phi : G \times X \to X$ such that

$$\phi(1, x) = x \quad \forall x \in X, \quad \phi(g, \phi(h, x)) = \phi(gh, x) \quad \forall g, h \in G, \ x \in X.$$

In the context of $T-$periodic loops in $\mathcal{X}$, we can describe the action of a finite group G by defining how its elements behave on the space, time and body labels. More precisely, given $x \in \Lambda$ and $t \in \mathbb{T}$, it is possible to represent the action of an element $g \in G$ over $x(t)$ through the following homomorphisms

$$\rho : G \to O(d), \quad \tau : G \to O(2), \quad \sigma : G \to \Sigma_n,$$

where $O(d)$ and $O(2)$ denote the orthogonal groups of dimension d and 2 respectively, and Σ_n is the group of all permutations of n objects labelled in $\{1, \dots, n\}$.

In practice, given $g \in G$, $\rho(g)$ describes how g acts on the $d-$dimensional space where every x_i lies, while $\sigma(g)$ describes the possible interchanging of bodies along the loop. As for $\tau(g)$, it is used to represent possible symmetries or recurrences of the orbit over a period T. In Section 3, a group G will be identified by its generators, whose representations on $O(d), O(2)$ and Σ_n will be provided.

Given a finite group G, we can define the set of the (possibly colliding) *G-equivariant* loops in Λ as the sets

$$\Lambda^G = \{x \in \Lambda \ : \ (gx)(t) = x(t), \ \forall t \in \mathbb{T}, \ g \in G\},$$
$$\hat{\Lambda}^G = \left\{x \in \Lambda^G \ : \ x \in \hat{\Lambda}\right\}$$

that is, the set of all elements of Λ (resp. $\hat{\Lambda}$) which are invariant under the action of G. It is possible to show (see Barutello et al., 2026, Lemma 2.4) that, if $\bar{x} \in \hat{\Lambda}^G$ is a critical point of the restriction $\mathcal{A}_{|_{\Lambda^G}}$, then it is a critical point of $\mathcal{A}$ over the whole Λ, and hence a periodic G-equivariant solution of (1). With suitable constraints on G, one can ensure *a priori* the existence of such collision-less critical points (see again (Ferrario and Terracini, 2004; Barutello et al., 2026) for more details).

To find critical points of $\mathcal{A}_{|_{\Lambda^G}}$, it is possible to operate a further reduction by considering a particular subinterval $\mathbb{I} \subset \mathbb{T}$, called the *fundamental domain*. In short, the fundamental domain $\mathbb{I}$ is such that

(A) defined $\bar{G} = G/\ker\tau$, one has

$$\mathbb{T} = \bigcup_{[g]\in\bar{G}} \tau(g^{-1})\mathbb{I}, \quad |\mathbb{I}| = \frac{|\mathbb{T}|}{|\bar{G}|}$$

(B) if $\bar{y} : \mathbb{I} \to \mathcal{X}$ is a critical point of the restricted action

$$\mathcal{A}_{\mathbb{I}}(y) = \int_{\mathbb{I}} L(y(t), \dot{y}(t))dt$$

over a suitable set of fixed-ends trajectories, then the symmetrised path given by the concatenation of $g\bar{y}$, $g \in \bar{G}$, is a solution of the $G-$equivariant $n-$body problem (see Barutello et al., 2026, Theorem 3.2).

Some considerations on properties (A) and (B) are in order to understand the optimisation process and, later on, the computation of the stability indicators. Property (A) claims that it is possible to re-construct the whole period simply looking at the action of $\tau(G)$ on the segment $\mathbb{I}$. As for property (B), it allows to restrict our search for critical points of the action in the set of segments of our $T-$periodic orbits with suitable constraints at the endpoints. In particular, y must belong to a class Y of fixed-ends-type paths whose precise definition depends on the form of $\tau(G)$ (see Barutello et al., 2026, Proposition 3.1). Without loss of generality, we will take $\mathbb{I} = [0, \pi]$ and $T = l\pi$, $l \in \mathbb{N}$.

The optimisation of the restricted action functional $\mathcal{A}_{\mathbb{I}}$ is the key problem tackled by the numerical algorithm, which is the core of *SymOrb.jl*. Given a symmetry group, and, consequently, the corresponding fundamental domain $\mathbb{I}$ and the set of the paths Y, the routine takes advantage of a wide variety of optimisation and refinement methods to compute an approximation of a critical point $\bar{y}$ of $\mathcal{A}_{\mathbb{I}}$ over Y as a truncated Fourier series added to a linear interpolation between the boundary configurations:

$$y(t) = y_0 + \tfrac{t}{\pi}(y_1 - y_0) + \sum_{k=1}^{F} a_k \sin(kt), \quad t \in [0, \pi]. \tag{3}$$

Finally, by symmetrising $\bar{y}$, an approximated solution $\bar{x}$ of (1) over the period T is obtained and can be expressed as a truncated Fourier series

$$\bar{x}(t) = A_0 + \sum_{k=1}^{\bar{F}} A_k \cos\left(k\tfrac{2\pi}{T}t\right) + \sum_{k=1}^{\bar{F}} B_k \sin\left(k\tfrac{2\pi}{T}t\right), \quad t \in [0, T]. \tag{4}$$

The coefficients A_0, A_k, B_k are computed analytically from the a_k as shown in Appendix.

The output of the optimisation is provided in two ways: first, the Fourier coefficients of $\bar{y}$ on $\mathbb{I}$, and secondly, the pointwise representation of $\bar{x}$ on $\mathbb{T}$.

Once the approximated solution is provided, one can proceed with its stability analysis, which is the topic of next Section.

2. Stability indicators

Once an approximated solution of (1) is obtained via the *SymOrb.jl* algorithm, it is possible to study its stability as a periodic orbit of the $n-$body problem. In this section, we will propose two different ways to evaluate stability. First of all, we will define the Floquet multipliers, that can be used to evaluate the change rate of a periodic orbit under small changes in its initial condition. Secondly, we will introduce the Morse index, which is related to the variation of the Lagrangian action value when the orbit is slightly deformed. For both quantities, we will provide the basic definitions and the computing methods in our context; the interested can find more details on such stability indicators in Teschl (2012, Chapters 3 and 12), Morse (1934), Smale (1965), as well as other applications of index theory to problems in celestial mechanics in Ambrosetti and Coti Zelati (1993), Rabinowitz (1978), Barutello et al. (2020).

2.1. Floquet multipliers

Let us start by taking a general ordinary nonlinear differential equation of the form

$$\dot{x}(t) = f(x(t)) \tag{5}$$

where $x : \mathbb{R} \to \mathbb{R}^N$, for some $N \geq 1$ and $f : \mathbb{R}^N \to \mathbb{R}^N$. Suppose that the above system admits a $T-$periodic solution, $T > 0$, denoted by $\bar{x}(t)$. The linear stability of such periodic solution can be analysed by passing to the linearised system

$$\dot{y}(t) = A_{\bar{x}}(t)y(t), \ A_{\bar{x}}(t) = Df(\bar{x}(t)) \ : \tag{6}$$

clearly, $A_{\bar{x}}(t)$ is a periodic $N \times N$ matrix and depends on the particular solution $\bar{x}(t)$. Following the theory of periodic linear systems, it is possible to define the *principal matrix solution* X as the unique solution of the differential system

$$\begin{cases} \dot{X}(t) = A_{\bar{x}}(t)\, X(t) \\ X(0) = I_N, \end{cases} \tag{7}$$

where $X(t) \in \mathbb{R}^{N\times N}$ for every $t \in \mathbb{R}$ and I_N is the $N-$dimensional identity. Starting from $X(t)$ one can define the *Monodromy matrix* related to problem (6) as $\mathcal{M}_{\bar{x}} = X(T)$.

The spectral properties of the monodromy matrix are related to the linear stability of the periodic solution $\bar{x}$: if all eigenvalues of $\mathcal{M}_{\bar{x}}$ have complex modulus less or equal to 1, then $\bar{x}$ is *linearly stable*. Otherwise, $\bar{x}$ is *linearly unstable*. The eigenvalues of $M_{\bar{x}}$ are called the *Floquet multipliers* associated to the orbit $\bar{x}$ (see, for instance, Teschl, 2012, Theorem 12.4 Barutello et al., 2016b and Calleja et al., 2021).

It is important to note that the analytical computation of Floquet multipliers is, in general, a challenging task, with only a limited number of known results. As a result, numerical methods are typically preferred for their determination (see the next sections for references in the case of n-body problem).

2.1.1. Computation of Floquet multipliers for the $n-$body problem

Following previous works in the literature (see, e.g., Vanderbei, 2004a; Barutello et al., 2016b; Calleja et al., 2021), we analyse the stability of solutions in terms of Floquet multipliers for Problem (1), after rewriting it as the following first-order system of ODEs

$$\begin{cases} \dot{x} = M^{-1}\, y, \\ \dot{y} = \nabla U(x), \end{cases} \tag{8}$$

where $M^{-1} \in \mathbb{R}^{d\times n}$ is the inverse of the diagonal block-matrix

$$M^{-1} = \begin{bmatrix} m_1\, I_n & 0 & 0 \\ 0 & m_2\, I_n & 0 \\ & \ddots & \\ 0 & & m_d\, I_n \end{bmatrix}$$

In this case, (7) should be read with $A_{\bar{x}}$ the following block-matrix $\mathbb{R}^{(d\times n)^2}$:

$$A_{\bar{x}}(t) = \begin{bmatrix} 0 & M^{-1} \\ \nabla^2 U(\bar{x}(t)) & 0 \end{bmatrix}$$

where $0 = 0_{\mathbb{R}^{d\times n}}$ and $\nabla^2 U$ is the Hessian matrix of the potential U computed along the periodic solution $\bar{x}(t)$.

In the context of mechanical systems, the monodromy matrix $\mathcal{M}_{\bar{x}}$ possesses the property that $\det(\mathcal{M}_{\bar{x}}) = 1$; this implies that for every (complex) eigenvalue z with modulus $|z| = r$, there exists another eigenvalue w such that $|w| = 1/r$. As a result, an orbit $\bar{x}$ is stable if and only if the spectrum of $\mathcal{M}_{\bar{x}}$ is entirely contained within the unit circle $\{|z| = 1\}$ in the complex plane.

The following algorithm is proposed for reckoning the discrete Floquet stability of an orbit.

Algorithm 1 Floquet Algorithm

1: **Input:** The periodic orbit, expressed in terms of its (truncated) Fourier coefficients (see (4)).
2: **Output:** The eigenvalues of the monodromy matrix.
3: **Step 1.** Build the Hessian matrix $\nabla^2 U(\bar{x}(t))$
4: **Step 2.** Define the matrix differential equation (7)
5: **Step 3.** Compute the principal solution matrix $X(t)$
6: **Step 4.** Compute the complex eigenvalues of $\mathcal{M}_{\bar{x}} = X(T)$

In Section 3, we will apply the above algorithm to ten test cases, corresponding to orbits in the plane or the three-dimensional space with a variable number of bodies.

2.2. Discrete Morse index

The second stability indicator we propose is the *Morse index*, which measures the number of independent directions along which the action functional decreases, thus distinguishing minima, saddles, and unstable configurations within a variational framework (Morse, 1934; Smale, 1965).

For numerical studies of periodic orbits and choreographies, the Morse index serves as a practical diagnostic tool, allowing one to detect bifurcations and qualitative changes in stability (Fukuda et al., 2018, 2019; Barutello et al., 2016a). Its discrete formulation, following the combinatorial approach of Forman (1998), adapts these ideas to finite-dimensional settings, where the action is defined on a discretised configuration space.

Following Ciccarelli et al. (2025), we can give the following general definition.

Definition 1 (*Computational Discrete Morse Index*)**.** Let $f : H \to \mathbb{R}$ be a C^2 function and p a non-degenerate critical point of f. The *index* of p is defined as the dimension of the maximal subspace of the tangent space at p where the Hessian is negative definite. Consequently, the *discrete Morse index* $\tilde{n}^-$ of p is the number of negative eigenvalues of the Hessian matrix $H_f(p)$.

In summary, the discrete Morse index provides a numerical way to distinguish between different types of critical points: minima satisfy $\tilde{n}^-(p) = 0$, while saddle points correspond to $\tilde{n}^-(p) > 0$.

2.2.1. Application to the n-body problem

In the context of the n-body problem, the computation of the discrete Morse index requires first the discretisation of the action functional. This preliminary step transforms the continuous variational problem into a finite-dimensional optimisation problem, whose critical points approximate periodic orbits of the system. Once the action functional has been discretised, the Morse index can then be evaluated either on the *fundamental domain* $\mathbb{I}$ or, by exploiting the symmetries of the orbit, on the *entire domain*. Clearly, the index computed on the fundamental domain does not exceed that obtained over the full orbit.

Discretisation of the action functional. Following dlfer (2017), the action functional (2) can be discretised in two main ways.

Point discretisation. In this approach, the integral is approximated by quadrature on a uniform grid $0 = t_0 < t_1 < \cdots < t_{M+1} = T$. Derivatives are replaced with finite differences, and the action is written in terms of the discrete variables $y_i^k \approx x_i(t_k) \in \mathbb{R}^d$, for $i = 1, \dots, n$ and $k = 0, \dots, M+1$. This yields the discrete functional

$$f_1(y_i^k) = \mathcal{A}_h^{(1)}, \tag{9}$$

defined on the block matrix $(y_i^k)_{i,k} \in \mathbb{R}^{d\times n\times(M+2)}$. For details see Cravero and Introna (2024), dlfer (2017).

Fourier coefficients discretisation. Alternatively, the trajectory is approximated by a truncated Fourier series as in (3) and (4). Substituting into (2) gives

$$f_2(x_0, x_1, A_k) = \mathcal{A}_h^{(2)}. \tag{10}$$

The variables are the endpoints and Fourier coefficients, with dimension $(F + 2) \times d \times n$. See dlfer (2017), Simó (2001b,c) for further discussion.

In both schemes, the problem reduces to optimising an objective function $f = f_i$ $(i = 1, 2)$ with respect to the chosen discrete variables, whose critical points correspond to periodic solutions of the system. Once a discrete periodic orbit has been obtained, one can further characterise the nature of the corresponding critical point by computing its discrete Morse index. This can be done in two equivalent settings, depending on whether one exploits the symmetries of the solution or not: either on the fundamental domain, where only a representative segment of the orbit is considered, or on the full orbit, where the computation is performed over the entire period.

On the fundamental domain. As described in Barutello et al. (2026), Ciccarelli et al. (2025), the Hessian of the discretised action functional can be computed within the fundamental domain $\mathbb{I}$ either by using a Fourier-based discretisation, where the trajectory is approximated by truncated series, or by direct pointwise discretisation, where the time interval is subdivided into a finite number of nodes.

On the full orbit. Alternatively, the discrete Morse index can be computed on the full periodic orbit. In this case, the action functional is discretised over the entire period, ensuring that periodic boundary conditions are satisfied. Since a periodic orbit has identical initial and final points, only one of them is retained in the computation.

2.2.2. Algorithm

The following procedure summarises the computation of the discrete Morse index on the entire orbit.

It is worth noting that, in contrast to previous studies that analysed specific families of solutions (such as the figure-eight choreography Chenciner and Montgomery, 2000), the approach adopted here is formulated to be applicable to any periodic orbit obtained numerically. In this way, the abstract concepts introduced earlier are translated into general computational tools, establishing a direct connection between the theoretical framework and the analysis of stability in the n-body problem.

2.3. Variational and dynamical stability

Our numerical results (see Section 3) emphasise, through a study on stability indicators, a well-known distinction between variational stability, described, in our case, by the Morse index of the Lagrangian action, and dynamical (linear) stability, measured by Floquet multipliers. Indeed, these are two different notions that, in general, do not coincide for the same orbit, as illustrated by several examples in this paper and in previous studies.

Algorithm 2 Computation of the Discrete Morse Index

1: **Input:** Periodic solution given either

   (a) by its Fourier coefficients (see (4)), or
   (b) by sampled positions $x_i(t_k)$ for each body $i = 1, \dots, n$ at times t_k, $k = 1, \dots, w$.

2: **Output:** Discrete Morse index $\tilde{n}^-(p)$.
3: **Step 1.** Build the Hessian matrix of the discretised action functional:

   • Fourier case: compute the Hessian in coefficient space.
   • Pointwise case: assemble the Hessian from the discretised action.

4: **Step 2.** Compute all eigenvalues λ_j of the Hessian.
5: **Step 3.** The discrete Morse index is the number of negative eigenvalues:

$$\tilde{n}^-(p) = \#\{\lambda_j < 0\}.$$

Variational stability concerns the behaviour of the action under a restricted class of perturbations, for example after imposing symmetries or after slightly deforming the orbit. A zero Morse index means that the orbit is a local minimiser of the action within this restricted setting.

On the other hand, dynamical stability describes how the orbit behaves under all small perturbations through the linearised equations of motion, including those that break the variational constraints. For this reason, unstable behaviours may take place even when the action has a local minimum, since they are not detected by the second variation of the action.

An example that clearly highlights this distinction is provided by the Lagrange equilateral triangle (Fig. 1). For the Newtonian 3-body problem with equal masses, the equilateral triangle is a minimising solution of the Lagrangian action among all periodic curves with the same symmetry constraints. This is confirmed by its zero Morse index. On the other hand, the computation of Floquet multipliers shows that this solution is linearly unstable, since some multipliers have modulus significantly larger than one. Indeed, the instability arises from perturbations that are not taken into account in the constrained variational problem, but are still present in the full dynamics. This explains how an action minimiser can nevertheless be linearly unstable.

Another example is given by the figure-eight solution (Fig. 3), which illustrates the opposite phenomenon. In this case, the orbit is not a minimiser of the action and has a positive Morse index. However, the Floquet spectrum lies close to the unit circle, indicating near linear stability. This behaviour can be explained by the strong symmetries of the orbit, which eliminate many unstable perturbations and make the linearised system highly degenerate. As a result, the remaining perturbations increase the action without leading to rapid dynamical instability.

The numerical results presented in the next section thus confirm the theoretical foundations stating that being a minimiser of the action is neither necessary nor sufficient for linear stability, even in highly symmetric settings.

Comparison with Morse index computations. Only a limited number of works address the computation of Morse indices for periodic solutions of the three-body problem, and most of the available results are obtained through analytical or semi-analytical methods rather than direct numerical evaluation of the second variation of the action. A direct correspondence can nevertheless be established between the discrete Morse indices computed in the present work and the Morse indices for the figure-eight choreography previously obtained by Fukuda et al. (2018, 2019). In that setting, the second variation of the action is analysed through the spectral properties of the continuous Hessian operator, and three distinct Morse indices are introduced, depending on the class of admissible variations: the full periodic Morse index N, the choreographic Morse index N_c, and the figure-eight choreographic Morse index N_e. For the Newtonian figure-eight solution, they report $N = 2$, while $N_c = N_e = 0$, indicating that the orbit is a saddle point of the unrestricted action functional, but a local minimiser when variations are constrained to respect choreographic and figure-eight symmetries. Our numerical results are in full agreement with this structure. When the Morse index is computed on the full period, we obtain a positive index equal to two, corresponding to unstable directions that break the choreographic symmetry. Conversely, when the computation is restricted to the fundamental domain associated with the figure-eight symmetry, the discrete Morse index vanishes, showing that no negative directions remain within the symmetric subspace. This agreement confirms that the discrete Hessian of the discretised action correctly captures the symmetry-dependent variational properties of the figure-eight choreography and provides a consistent finite-dimensional approximation of the corresponding continuous Morse index theory. A closely related phenomenon appears for other highly symmetric periodic solutions of the three-body problem. In particular, the Morse index of the Lagrangian circular orbit has been computed analytically by Barutello et al. (2016b), who showed that this relative equilibrium is, in general, a saddle point of the Lagrangian action functional on the full loop space, while it becomes a minimiser only when suitable constraints or invariant subspaces are imposed. Moreover, they demonstrated that transitions in linear stability are accompanied by jumps in the Morse index of the orbit and of its iterates. This behaviour closely parallels what is observed for the figure-eight choreography, where unstable directions exist in the unrestricted variational setting but disappear when symmetry restrictions are enforced.

3. Numerical results

This Section presents the application of the algorithms described in Section 2 to a set of ten distinct periodic orbits computed using *SymOrb.jl*. Figs. 1–10 display a wide variety of examples, including both planar and spatial configurations, and involving different numbers of bodies. For each orbit, we report:

- the generators of the finite symmetry group G associated with the orbits; recall that $\bar{G} = G/\ker\tau$ (see Section 1), and that the notation $R(\theta)$ denotes the rotation matrices of the form

$$R(\theta) = \begin{pmatrix} \cos\theta & -\sin\theta \\ \sin\theta & \cos\theta \end{pmatrix};$$

- the values of the action $\mathcal{A}$ and its gradient, to assess the accuracy of the numerical method in locating a critical point of $\mathcal{A}$;
- the numerical Morse index, computed both on the fundamental domain $\mathbb{I}$ and over the entire period; whenever this index is non-zero, we additionally report the maximal negative eigenvalue of $Hess(\mathcal{A})$;
- the largest modulus of the eigenvalues of the monodromy matrix, i.e., the maximal Floquet multiplier.

In the variational framework of the Morse index, the maximal negative eigenvalue provides a quantitative indication on how clearly the negative spectrum is separated from zero, and thus on the reliability of the computed Morse index. Conversely, in the Floquet analysis, the focus lies on the maximal (in modulus) eigenvalue of the monodromy matrix: when it lies far from ± 1, we can confidently conclude that the orbit, though numerical approximated, is linearly unstable.

The selected set of orbits is designed to represent the diversity of periodic solutions we can find in the $n-$body problem, with particular attention to non-collisional examples.

A notable subset consists in the so-called *choreographies*, where all bodies move along a common trajectory, as in Figs. 1, 3, and 5.

Group generator(s)	$\ker\tau = \langle \mathrm{Id} \rangle, \quad \bar{G} = \langle r \rangle$ $\rho(r) = -\mathrm{Id}, \quad \sigma(r) = ()$	
Action value		9.8022
Gradient norm		7.72×10^{-11}
Morse (fund. domain)	Index	0
	Max negative eigenvalue	—
Morse (period)	Index	0
	Max negative eigenvalue	—
Floquet	Norm of the max eigenvalue	85.021

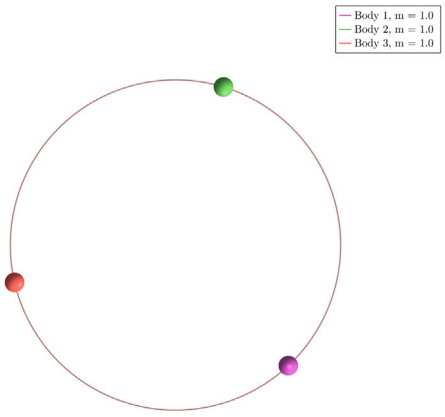

Fig. 1. Lagrange equilateral triangle. This orbit is a minimiser of the action, with zero Morse index, but exhibits linear instability, as indicated by Floquet multipliers with modulus larger than one.

Group generator(s)	$\ker\tau = \langle \mathrm{Id} \rangle, \quad \bar{G} = \langle r \rangle$ $\rho(r) = -\mathrm{Id}, \quad \sigma(r) = ()$	
Action value		10.937
Gradient norm		6.77×10^{-11}
Morse (fund. domain)	Index	1
	Max negative eigenvalue	-5.5278
Morse (period)	Index	3
	Max negative eigenvalue	-13.951
Floquet	Norm of the max eigenvalue	5.8982×10^{4}

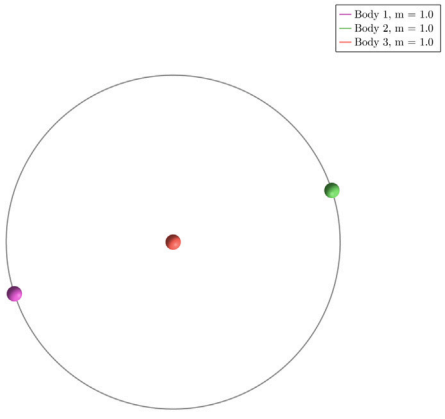

Fig. 2. Collinear relative equilibrium. This orbit is a linearly unstable collinear periodic solution of the 3-body problem, as indicated by its Floquet multipliers.

Group generator(s)	$\ker\tau = \langle \mathrm{Id} \rangle, \quad \bar{G} = \langle r, s \rangle$ $\rho(r) = \mathrm{Id}, \quad \sigma(r) = (1,2,3)$ $\rho(s) = -\mathrm{Id}, \quad \sigma(s) = (2,3)$	
Action value		5.8584
Gradient norm		4.85×10^{-12}
Morse (fund. domain)	Index	0
	Max negative eigenvalue	—
Morse (period)	Index	2
	Max negative eigenvalue	-0.22568
Floquet	Norm of the max eigenvalue	1.0187

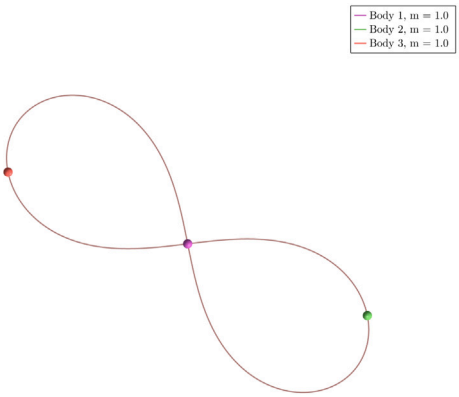

Fig. 3. Figure-eight choreography. The orbit is not a minimiser of the action and has positive Morse index, but its Floquet multipliers lie close to the unit circle, indicating near-linear stability.

Group generator(s)	$\ker\tau = \langle \mathrm{Id} \rangle, \quad \bar{G} = \langle r \rangle$ $\rho(r) = -\mathrm{Id}, \quad \sigma(r) = ()$	
Action value		10.442
Gradient norm		3.22×10^{-8}
Morse (fund. domain)	Index	0
	Max negative eigenvalue	—
Morse (period)	Index	2
	Max negative eigenvalue	-0.061729
Floquet	Norm of the max eigenvalue	1.0462

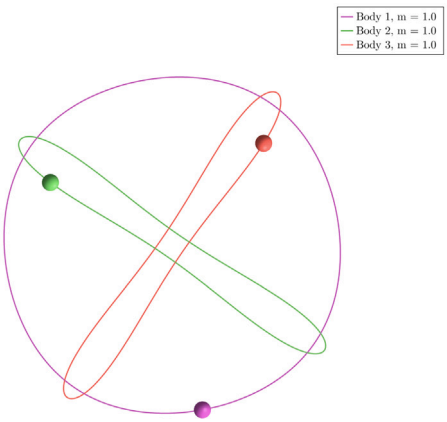

Fig. 4. Solution of the 3-body problem, typically known as *Ducati* and first discovered in Moore (1993). Its Floquet multipliers show that the orbit is linearly stable.

Group generator(s)	$\ker\tau=\langle \mathrm{Id}\rangle,\quad \bar{G}=\langle r\rangle$ $\rho(r)=\mathrm{Id},\quad \sigma(r)=(1,2,3,4,5,6,7,8,9,10,11,12)$	
Action value		72.621
Gradient norm		2.01×10^{-8}
Morse (fund. domain)	Index	0
	Max negative eigenvalue	—
Morse (period)	Index	4
	Max negative eigenvalue	-0.11029
Floquet	Norm of the max eigenvalue	4.1930×10^{12}

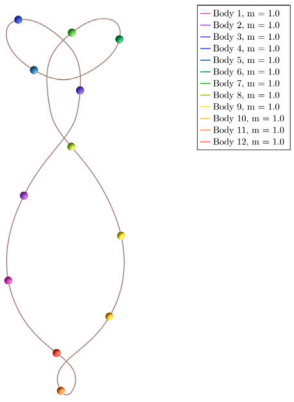

Fig. 5. Linearly unstable choreography of the 12-body problem.

Group generator(s)	$\ker\tau=\langle \kappa\rangle,\quad \bar{G}=\langle r\rangle$ $\rho(\kappa)=R(2\pi/5),\ \sigma(\kappa)=(1,2,3,4,5)(6,7,8,9,10)$ $\rho(r)=-\mathrm{Id},\quad \sigma(r)=()$	
Action value		114.33
Gradient norm		4.11×10^{-7}
Morse (fund. domain)	Index	0
	Max negative eigenvalue	—
Morse (period)	Index	2
	Max negative eigenvalue	-2.4157×10^{-3}
Floquet	Norm of the max eigenvalue	1174.0

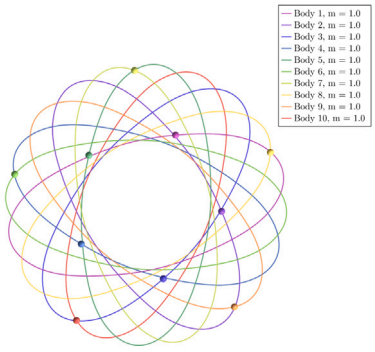

Fig. 6. Linearly unstable periodic solution of the 10-body problem.

Group generator(s)	$\ker\tau=\langle \mathrm{Id}\rangle,\quad \bar{G}=\langle r\rangle$ $\rho(r)=\begin{pmatrix}R(2\pi/3) & 0\\ 0 & -1\end{pmatrix},\quad \sigma(r)=()$	
Action value		8.3409
Gradient norm		3.46×10^{-8}
Morse (fund. domain)	Index	1
	Max negative eigenvalue	-3.0423
Morse (period)	Index	19
	Max negative eigenvalue	-48.541
Floquet	Norm of the max eigenvalue	6.3110×10^{8}

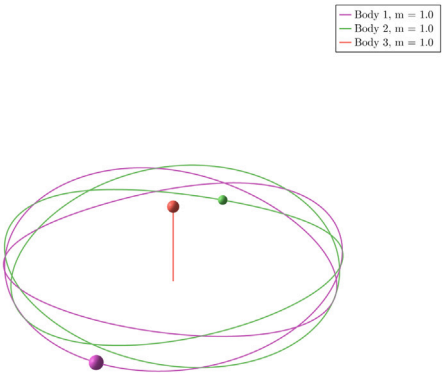

Fig. 7. Linearly unstable periodic solution of the spacial isosceles 3-body problem.

Group generator(s)	$\ker\tau=\langle \mathrm{Id}\rangle,\quad \bar{G}=\langle r,s\rangle$ $\rho(r)=-\mathrm{Id},\quad \sigma(r)=()$ $\rho(s)=\begin{pmatrix}-Id_2 & 0\\ 0 & 1\end{pmatrix},\quad \sigma(s)=()$	
Action value		11.900
Gradient norm		2.52×10^{-8}
Morse (fund. domain)	Index	0
	Max negative eigenvalue	—
Morse (period)	Index	9
	Max negative eigenvalue	-11.632
Floquet	Norm of the max eigenvalue	25.174

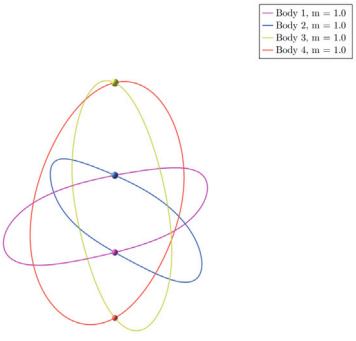

Fig. 8. Linearly unstable periodic solution of the 4-body problem.

Moreover, Figs. 1–4 correspond to classical solutions already studied in the literature (see, e.g., Barutello et al., 2016b; Roberts, 2002; Simó, 2001a; Roberts, 2007; Vanderbei, 2004b), included here to facilitate comparison between our computations and known results. In particular, Fig. 2 shows a *collinear relative equilibrium*, a well-known solution whose first study traces back to early works such as Mayer (1933).

Group generator(s)	$\ker\tau = \langle \mathrm{Id} \rangle, \quad \bar{G} = \langle r, s \rangle$ $\rho(r) = -\mathrm{Id} \quad \sigma(r) = (1,2)(3,4)$ $\rho(s) = \begin{pmatrix} -\mathrm{Id}_2 & 0 \\ 0 & 1 \end{pmatrix} \quad \sigma(s) = ()$	
Action value		12.143
Gradient norm		5.27×10^{-10}
Morse (fund. domain)	Index	0
	Max negative eigenvalue	—
Morse (period)	Index	11
	Max negative eigenvalue	-202.18
Floquet	Norm of the max eigenvalue	2191.6

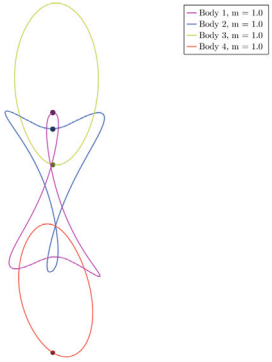

Fig. 9. Linearly unstable periodic solution of the 4-body problem.

Group generator(s)	$\ker\tau = \langle \mathrm{Id} \rangle, \quad \bar{G} = \langle r \rangle$ $\rho(r) = R(\pi/6)$ $\sigma(r) = (1,2,3,4,5,6,7,8,9,10,11,12)$	
Action value		81.641
Gradient norm		7.65×10^{-9}
Morse (fund. domain)	Index	0
	Max negative eigenvalue	—
Morse (period)	Index	4
	Max negative eigenvalue	-0.17774
Floquet	Norm of the max eigenvalue	8.5410×10^{12}

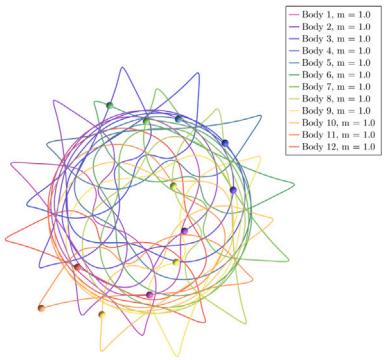

Fig. 10. Linearly unstable periodic solution of the 12-body problem.

Among our findings, it is worth noticing that the triangular Lagrange solution (Fig. 1) minimises the action functional, despite being linearly unstable. Conversely, the celebrated figure-eight choreography (Fig. 3) is not a minimiser of the action functional over its full period, yet it exhibits substantial linear stability – in agreement with previous studies (Simó, 2001a; Roberts, 2007; Galán-Vioque et al., 2005; Kapela and Simó, 2007).

Overall, our results illustrate the rich interplay between the variational and dynamical features of periodic orbits in the n-body problem. The comparison between Morse index (reflecting the local behaviour of $\mathcal{A}$ as a variational functional) and Floquet multipliers (characterising linear stability) reveals a wide spectrum of behaviours, which may serve as a useful tool for classifying and distinguishing periodic solutions according to their shared dynamical properties.

3.1. Implementation details and sensitivity analysis

As previously stated, all orbits were initially computed using `SymOrb.jl`.

A notable difference from the version presented in Barutello et al. (2026) (corresponding to Git commit `9ef31f3` of DipMathUniTO, 2024) is the introduction of two enhanced integration algorithms to compute the potential part of the action, its gradient, and its Hessian. The first algorithm, from `FastGaussQuadrature.jl`, employs Gauss–Legendre quadratures. It is used to improve the convergence of the optimisation procedure compared to the Trapezoidal method, without increasing computational complexity. The second algorithm is an implementation of adaptive Gauss–Kronrod quadratures provided by `QuadGK.jl`. This method adaptively subdivides the integration domain and recursively performs integration until a relative error tolerance of tol $= \sqrt{\epsilon}$ is met, where $\epsilon \approx 2.22\times10^{-16}$ is the machine epsilon.[2] Since this method is noticeably slower than the former one, it is used exclusively to improve the resolution of the found orbit and to precisely compute the indices.

The monodromy equation was integrated using the Julia package `DifferentialEquations.jl` (Rackauckas and Nie, 2017) via the `Tsit5` algorithm, a Tsitouras 5/4 Runge–Kutta method with a free 4th-order interpolant.

Table 1 reports two distinct truncation orders, F and $\tilde{F}$. The former, F, refers to the representation of the orbit on the fundamental domain and it was initially set at $F_1 = 24$ to identify the orbits and compute the corresponding results. To ensure the correctness of these findings, the orbits were subsequently refined using $F_2 = 36$, $F_3 = 48$ and $F_4 = 96$ modes, and the computations were repeated for verification. The latter, $\tilde{F}$, refers to the truncation order for the full period $T = m\pi$, where m is the order of the symmetry group. It is chosen to be $\tilde{F} = m \cdot F$, to avoid losing orbital features.

The results displayed in Figs. 1–10 correspond to the initial truncation order F_1 and $\tilde{F}_1$, while the complete data for all cases are presented in Table 1.

We highlight that calculating the Morse index and Floquet multipliers requires finding the eigenvalues of potentially large matrices. In this work, we used built-in Julia functions (based on LAPACK and BLAS routines) to compute the full spectrum of eigenvalues for matrices with dimensions that scale linearly with both the truncation order and the number of bodies. Note that the results for Orbit 5 and Orbit 10 are reported only for $\tilde{F}_1 = 288$ and $\tilde{F}_2 = 432$ Fourier modes since the available RAM was insufficient to handle the periodic orbit computations for the higher resolutions of $\tilde{F}_3 = 576$ and $\tilde{F}_4 = 1152$. This limitation could be addressed in future work by employing optimised or iterative algorithms.

Given the numerical nature of these spectral computations, we apply a threshold to distinguish physical instability from numerical

[2] For all results presented, computations were performed using Julia 1.12 on a notebook equipped with 16 GB of RAM, Intel® Core™ Ultra 7 155H, running Arch Linux.

Table 1
Comparison of the results where respectively 24, 48, and 96 Fourier modes are taken into account.

	F	$\tilde{F}$	Morse (fund. domain)		Morse (period)		Floquet
			Index	Max. neg. eig.	Index	Max. neg. eig.	
Orbit 1	24	48	0	–	0	–	85.021
	36	72	0	–	0	–	85.020
	48	96	0	–	0	–	85.020
	96	192	0	–	0	–	85.020
Orbit 2	24	72	1	−5.5278	3	−13.951	5.8982×10^4
	36	72	1	−5.5278	3	−13.950	5.8980×10^4
	48	96	1	−5.5279	3	−13.950	5.8978×10^4
	96	192	1	−5.5279	3	−13.950	5.8978×10^4
Orbit 3	24	48	0	–	2	−0.22568	1.0187
	36	108	0	–	2	−0.22568	1.0102
	48	144	0	–	2	−0.22568	1.0066
	96	288	0	–	2	−0.22568	1.0066
Orbit 4	24	48	0	–	2	−0.061729	1.0462
	36	72	0	–	2	−0.061853	1.0254
	48	96	0	–	2	−0.061903	1.0166
	96	192	0	–	2	−0.061904	1.0230
Orbit 5	24	288	0	–	4	−0.11029	4.1930×10^{12}
	36	432	0	–	2	−0.11020	8.5482×10^{12}
	48	576	0	–	2	(failed)	(failed)
	96	1152	0	–	2	(failed)	(failed)
Orbit 6	24	48	0	–	2	-2.4157×10^{-3}	1174.0
	36	72	0	–	2	-2.4786×10^{-3}	1173.9
	48	96	0	–	2	-2.4999×10^{-3}	1173.9
	96	192	0	–	2	-2.4999×10^{-3}	1173.9
Orbit 7	24	144	1	−3.0423	19	−48.541	6.311×10^8
	36	216	1	−3.0423	19	−48.538	6.308×10^8
	48	288	1	−3.0423	19	−48.537	6.310×10^8
	96	576	1	−3.0423	19	−48.537	6.307×10^8
Orbit 8	24	48	0	–	9	−11.632	25.174
	36	72	0	–	9	−11.632	25.172
	48	96	0	–	9	−11.632	25.172
	96	192	0	–	9	−11.631	25.172
Orbit 9	24	48	0	–	11	−202.18	2191.6
	36	72	0	–	11	−266.60	1640.1
	48	96	0	–	11	−311.40	1166.4
	96	192	0	–	11	−311.40	1166.4
Orbit 10	24	288	0	–	4	−0.1778	8.5410×10^{12}
	36	432	0	–	11	−311.3904	8.5482×10^{12}
	48	576	0	–	11	(failed)	(failed)
	96	1152	0	–	11	(failed)	(failed)

noise. We consider an eigenvalue to be different from 0 (for the Morse index) or 1 (for the Floquet multiplier) if its distance to the relevant number is greater than the threshold 10^{-3}. In almost all the cases considered, this choice is more than sufficient to establish the stability.

3.2. Validation and comparison with known results

Among the orbits presented in this paper (corresponding to Figs. 1–10), the first four (namely, Figs. 1–4) correspond to known solutions, whereas the remaining ones (Figs. 5–10) represent, to the best of our knowledge, *new orbits*, exhibiting relatively good properties in terms of deep search and exploration of our algorithm. Consequently, for Figs. 5–10, the indices that we introduce cannot be validated against previously known results. For the known solutions shown in Figs. 1 and 3, the Morse index computations discussed in Section 2.3 already provide a validation, as they correctly reproduce the expected symmetry-dependent variational stability properties.

We now complement this analysis by comparing the remaining numerical stability indicators with analytical and numerical results available in the literature.

Figs. 1 and 2 correspond to classical solutions of the three-body problem, namely *relative equilibria*. In particular, Fig. 1 represents the *equilateral triangular* relative equilibrium, while Fig. 2 corresponds to a *collinear* relative equilibrium. Concerning linear stability—closely related to the Floquet index introduced in this work—the following facts are well known. For the three-body problem, collinear relative equilibria are linearly unstable for every choice of the masses (see, e.g., Roberts, 2002). This explains the large value of the Floquet index observed in Fig. 2.

The equilateral triangular configuration (Fig. 1) is also known to be linearly unstable in general, as established by the *Gascheau–Routh criterion*, which states that linear stability holds if and only if

$$27\,(m_1m_2 + m_1m_3 + m_2m_3) < (m_1 + m_2 + m_3)^2,$$

that clearly does not hold in the case $m_1 = m_2 = m_3 = 1$. Moreover, our outcome is in agreement with the results reported in Vanderbei (2004b, "Lagrange3" in Table 2).

We now turn to the orbits depicted in Figs. 3 and 4. The orbit shown in Fig. 3 was proven to be linearly stable in Kapela and Simó (2007), resolving a long-standing conjecture originally proposed by Simó, through a computer-assisted proof (see also Roberts, 2007; Vanderbei, 2004b). In our computations, the outcome depends on the numerical tolerance adopted, which is consistent with the delicate nature of the stability analysis for this orbit. This is also confirmed by the results presented in 1, where the modulus of the Floquet multiplier approaches 1 whenever the number of Fourier modes increases.

The orbit shown in Fig. 4 is referred to as the *"Ducati"* orbit in Vanderbei (2004b, "Ducati3" in Table 1), where its Floquet index is computed numerically. Our results are in good agreement with those findings.

Table 2
Validation of the numerical results for the orbits considered in this paper.

Figure	Validation method	Consistency
Figure 1	Classical analytical results	✓
Figure 2	Classical analytical results	✓
Figure 3	Theoretical and numerical results	✓
Figure 4	Numerical results	✓
Figures 5–10	No previous results (unknown orbits)	

These comparisons are summarised in Table 2.

Furthermore, checking again the results presented in Table 1, it is possible to observe as the outcomes, except for orbit 9, are particularly stable when varying the number of Fourier modes considered. As for orbit 9, a significant variation occurs only comparing $F = 24$ and $F = 48$, and without affecting the effective stability property of the orbit.

4. Conclusions and final remarks

Through this paper, we were able to show that the routine presented in *SymOrb.jl* can be used not only to find new orbits of the n-body problem (as shown in dlfer, 2017), but also to analyse their stability properties with results which are consistent with the literature. The landscape emerging from the results shows a variety of possible scenarios, where variational and linear stability need to be studied separately. As already mentioned in dlfer (2017) itself, the method used to find such orbits is purely variational, and in that it differs from the more common shooting method used in most cases to solve differential systems. This allows to focus the search on truly periodic orbits, fixing their symmetry properties through G-equivariance. The analysis we presented in the current paper has to be intended as a preliminary numerical study, that, besides being interesting *per se*, is a necessary first step for a systematic study on a vast catalogue of orbits. Indeed, Morse indices and Floquet multipliers can be used also as labels, which allow to discern different trajectories not only on the basis of their shape similarities, but also considering deeper dynamical features.

CRediT authorship contribution statement

Diego Berti: Writing – review & editing, Writing – original draft, Visualization, Validation, Supervision, Software, Resources, Project administration, Methodology, Investigation, Funding acquisition, Formal analysis, Data curation, Conceptualization. **Gian Marco Canneori:** Writing – review & editing, Writing – original draft, Visualization, Validation, Supervision, Software, Resources, Project administration, Methodology, Investigation, Funding acquisition, Formal analysis, Data curation, Conceptualization. **Roberto Ciccarelli:** Writing – review & editing, Writing – original draft, Visualization, Validation, Supervision, Software, Resources, Project administration, Methodology, Investigation, Funding acquisition, Formal analysis, Data curation, Conceptualization. **Irene De Blasi:** Writing – review & editing, Writing – original draft, Visualization, Validation, Supervision, Software, Resources, Project administration, Methodology, Investigation, Funding acquisition, Formal analysis, Data curation, Conceptualization. **Margaux Introna:** Writing – review & editing, Writing – original draft, Visualization, Validation, Supervision, Software, Resources, Project administration, Methodology, Investigation, Funding acquisition, Formal analysis, Data curation, Conceptualization. **Davide Polimeni:** Writing – review & editing, Writing – original draft, Visualization, Validation, Supervision, Software, Resources, Project administration, Methodology, Investigation, Funding acquisition, Formal analysis, Data curation, Conceptualization.

Declaration of generative AI in scientific writing

During the revision of this work the authors used LLMs to the sole scope of review the language. After using this tools, the authors reviewed and edited the content as needed and take full responsibility for the content of the publication. Built-in tools (such as GitHub Co-Pilot) have been used in the coding phase.

Funding

M.I. conducted this research during and with the support of the Italian national inter-university PhD programme in Space Science and Technology. Moreover M.I. is partially supported by INdAM group G.N.A.M.P.A.

I.D.B. is supported by the Italian Research Center on High Performance Computing Big Data and Quantum Computing (ICSC), project funded by European Union - NextGenerationUE and National Recovery and Resilience Plan (NRRP) - Mission 4 Component 2. Spoke 3, Astrophysics and Cosmos Observations. D. B. was supported by the project NODES which has received funding from the MUR – M4C2 1.5 of PNRR funded by the European Union – NextGenerationEU (Grant agreement no. ECS00000036). D. B. was partially supported by INdAM group G.N.A.M.P.A. D.P. is partially supported by INdAM group G.N.A.M.P.A.

Declaration of competing interest

The authors declare the following financial interests/personal relationships which may be considered as potential competing interests: Irene De Blasi reports financial support was provided by European Union. Irene De Blasi reports financial support was provided by Francesco Severi National Institute of Higher Mathematics.

Margaux Introna reports financial support was provided by Francesco Severi National Institute of Higher Mathematics National Group for Mathematical Analysis Probability and their Applications.

Gian Marco Canneori reports financial support was provided by Francesco Severi National Institute of Higher Mathematics National Group for Mathematical Analysis Probability and their Applications.

Davide Polimeni reports financial support was provided by Francesco Severi National Institute of Higher Mathematics National Group for Mathematical Analysis Probability and their Applications.

Diego Berti reports financial support was provided by European Union - NextGenerationEU, Mission 4 Component 2 - ECS00000036 - CUP D17G22000150001. Diego Berti reports financial support was provided by Francesco Severi National Institute of Higher Mathematics National Group for Mathematical Analysis Probability and their Applications. If there are other authors, they declare that they have no known competing financial interests or personal relationships that could have appeared to influence the work reported in this paper.

Acknowledgements

The authors thank Vivina Barutello, Susanna Terracini, Mattia G. Bergomi, Pietro Vertechi, Davide L. Ferrario.

Appendix. Fourier coefficients on the whole period from the ones on the fundamental domain

Let G be a finite group acting on the orbits as defined in Section 1 and associate to each $g \in G$ the matrix $M_g = \rho(g) \otimes p(\sigma(g))$, where $\otimes$ is the Kronecker product and p is the representation of the permutations on the orthogonal group. Consider an orbit $x(t)$ on the fundamental domain $\mathbb{I} = [0, \pi]$ as in (3) and let $\tilde{x}(t)$ be the orbit extended to the whole period T via the action of G as in (4). Its Fourier coefficients A_0, A_k, B_k are given by

$$\begin{aligned} A_0 &= \frac{1}{T}\int_0^T \tilde{x}(t)dt \\ A_k &= \frac{2}{T}\int_0^T \tilde{x}(t)\cos\left(\frac{2\pi}{T}kt\right)dt \\ B_k &= \frac{2}{T}\int_0^T \tilde{x}(t)\sin\left(\frac{2\pi}{T}kt\right)dt \end{aligned} \tag{A.1}$$

It is possible to solve the integrals analytically and compute A_0, A_k and B_k in terms of a_k. However, the results depend heavily on the structure of $\bar{G}$. As shown in Ferrario and Terracini (2004), there are only three possible cases, as $\bar{G}$ can be composed:

- solely of time rotations *("Cyclic action")*
- of a single time reflection *("Brake action")*
- of both time rotations and time reflections *("Dihedral action")*.

The Cyclic case requires separate treatment from the Brake and Dihedral cases.

For later convenience, let $p, q \in \mathbb{N}$ and let us define

$$c_q^p = \cos\left(\frac{p}{q}\pi\right), \qquad s_q^p = \sin\left(\frac{p}{q}\pi\right),$$

and the integrals

$$I = \int_0^\pi x(t)dt = \frac{\pi}{2}(x_0 + x_1) + \sum_{\substack{h=1\dots F \\ h \text{ odd}}} \frac{2a_h}{h}$$

$$\begin{aligned} (I_{\cos})_q^p &= \int_0^\pi x(t)\cos\left(\frac{pt}{q}\right)dt = \\ &= \begin{cases} \frac{q^2}{\pi p^2}(c_q^p - 1)(x_1 - x_0) + \frac{q}{p}s_q^p x_1 + \sum\limits_{\substack{h=1\dots F \\ p\neq qh}} \left[c_q^p - (-1)^h\right] H_{q,h}^p a_h & \text{if } p \neq q \\ \frac{2}{\pi}(x_0 - x_1) + \sum\limits_{\substack{h=1\dots F \\ h \text{ even}}} \frac{2ha_h}{h^2 - 1} & \text{if } p = q \end{cases} \\ (I_{\sin})_q^p &= \int_0^\pi x(t)\sin\left(\frac{pt}{q}\right)dt = \\ &= \begin{cases} \frac{q^2}{\pi p^2}s_q^p(x_1 - x_0) + \frac{q}{p}(x_0 - c_q^p x_1) + \sum\limits_{h=1\dots F} f_{q,h}^p a_h & \text{if } p \neq q \\ \frac{\pi}{2}a_1 + x_0 + x_1 & \text{if } p = q \end{cases} \end{aligned}$$

where

$$H_{q,h}^p = \frac{(-1)^h}{h\left[\left(\frac{p}{hq}\right)^2 - 1\right]}, \qquad f_{q,h}^p = \begin{cases} \frac{\pi}{2} & \text{if } h = \frac{p}{q} \\ s_q^p H_{q,h}^p & \text{otherwise.} \end{cases}$$

Cyclic action. If the action of $\bar{G}$ is cyclic, $\bar{G} = \langle g \rangle$ and $\tau(g^{-1})t = t + \pi$. Hence, the orbit extended to the whole period $T = m\pi$ via the action of G is

$$\tilde{x}(t) = (M_g)^l \cdot x(t - l\pi) \qquad \text{if } t \in [l\pi, (l+1)\pi]$$

and substituting into (A.1) we obtain

$$\begin{aligned} A_0 &= \frac{1}{m\pi}\sum_{l=0}^{m-1}\int_{l\pi}^{(l+1)\pi} \tilde{x}(t)dt = \frac{1}{m\pi}\sum_{l=0}^{m-1}(M_g)^l I \\ A_k &= \frac{2}{m\pi}\sum_{l=0}^{m-1}\int_{l\pi}^{(l+1)\pi} \tilde{x}(t)\cos\left(\frac{2kt}{m}\right)dt \\ &= \frac{2}{m\pi}\sum_{l=0}^{m-1}(M_g)^l\left[c_m^{2kl}(I_{\cos})_m^{2k} - s_m^{2kl}(I_{\sin})_m^{2k}\right] \\ B_k &= \frac{2}{m\pi}\sum_{l=0}^{m-1}\int_{l\pi}^{(l+1)\pi} \tilde{x}(t)\sin(\frac{2kt}{m})dt \\ &= \frac{2}{m\pi}\sum_{l=0}^{m-1}(M_g)^l\left[s_m^{2kl}(I_{\cos})_m^{2k} + c_m^{2kl}(I_{\sin})_m^{2k}\right]. \end{aligned}$$

Dihedral or brake action. If the action is dihedral or brake, $\bar{G} = \langle h_0, h_1 \rangle$ with h_i such that $\tau(h_0)t = -t$ and $\tau(h_1)t = 2\pi - t$. Defining $g = h_1 h_0$, its action on time is $\tau(g)t = \tau(h_1 h_0)t = \tau(h_1)\tau(h_0)t = 2\pi - (-t) = t + 2\pi$.

Hence we have

$$\tilde{x}(t) = \begin{cases} (M_g)^l \cdot x(t - 2l\pi) & t \in [2l\pi, (2l+1)\pi] \\ (M_g)^l M_{h_1} \cdot x\big((2l+2)\pi - t\big) & t \in [(2l+1)\pi, (2l+2)\pi] \end{cases} \qquad l = 0, \dots, m-1$$

Substituting into (A.1) we obtain

$$\begin{aligned} A_0 &= \frac{1}{2m\pi}\sum_{l=0}^{m-1}\int_{2l\pi}^{2(l+1)\pi} \tilde{x}(t)dt = \frac{1}{2m\pi}\sum_{l=0}^{m-1}(M_g)^l\left[Id + M_{h_1}\right] I \\ A_k &= \frac{2}{2m\pi}\sum_{l=0}^{m-1}\int_{2l\pi}^{2(l+1)\pi} \tilde{x}(t)\cos\left(\frac{kt}{m}\right)dt = \\ &= \frac{1}{m\pi}\sum_{l=0}^{m-1}(M_g)^l\left[c_m^{2kl}(I_{\cos})_m^k - s_m^{2kl}(I_{\sin})_m^k\right. \\ &\quad \left. + M_{h_1}\left(c_m^{2k(l+1)}(I_{\cos})_m^k + s_m^{2k(l+1)}(I_{\sin})_m^k\right)\right] \\ B_k &= \frac{2}{2m\pi}\sum_{l=0}^{m-1}\int_{2l\pi}^{2(l+1)\pi} \tilde{x}(t)\sin\left(\frac{kt}{m}\right)dt = \\ &= \frac{1}{m\pi}\sum_{l=0}^{m-1}(M_g)^l\left[s_m^{2kl}(I_{\cos})_m^k + c_m^{2kl}(I_{\sin})_m^k\right. \\ &\quad \left. + M_{h_1}\left(s_m^{2k(l+1)}(I_{\cos})_m^k - c_m^{2k(l+1)}(I_{\sin})_m^k\right)\right] \end{aligned}$$

Data availability

The data that support the findings of this study are available from the corresponding author upon reasonable request. They will deposited in a public repository after the end of the research project.

References

Ambrosetti, A., Coti Zelati, V., 1993. Periodic solutions of singular Lagrangian systems. In: Progress in Nonlinear Differential Equations and Their Applications, vol. 10, Birkhäuser, Basel, doi:10.1007/978-3-0348-8604-3.

Bahri, A., Rabinowitz, P.H., 1991. Periodic solutions of Hamiltonian systems of 3-body type. Ann. L'Institut Henri PoincarÉ C, Anal. Non Linéaire 8 (6), 561–649.

Barutello, V., Canneori, G.M., Ciccarelli, R., Terracini, S., Bergomi, M.G., Vertechi, P., Ferrario, D.L., 2026. Equivariant optimisation for the gravitational n-body problem: A computational factory of symmetric orbits. Commun. Nonlinear Sci. Numer. Simul. 152, 109180. doi:10.1016/j.cnsns.2025.109180.

Barutello, V., Hu, X., Portaluri, A., Terracini, S., 2020. An index theory for asymptotic motions under singular potentials. Adv. Math. 370.

Barutello, V., Jadanza, R.D., Portaluri, A., 2016a. Morse index and linear stability of the Lagrangian circular orbit in a three-body-type problem via index theory. Arch. Ration. Mech. Anal. 219 (1), 387–444. doi:10.1007/s00205-015-0898-2.

Barutello, V., Jadanza, R.D., Portaluri, A., 2016b. Morse index and linear stability of the Lagrangian circular orbit in a thre-bofy-type problem via index theory. Arch. Ration. Mech. Anal. 219, 387–444.

Barutello, V., Terracini, S., 2004. Action minimizing orbits in the n-body problem with simple choreography constraint. Nonlinearity 17 (6), 2015.

Bessi, U., Zelati, V.C., 1991. Symmetries and noncollision closed orbits for planar N-body-type problems. Nonlinear Anal. 16 (6), 587–598.

Boekholt, T.C.N., Portegies Zwart, S.F., Valtonen, M., 2020. Gargantuan chaotic gravitational three-body systems and their irreversibility to the Planck length. Mon. Not. R. Astron. Soc. 493 (3), 3932–3937. doi:10.1093/mnras/staa452.

Bolotin, S., 2006. Symbolic dynamics of almost collision orbits and skew products of symplectic maps. Nonlinearity 19 (9), 2041–2063. doi:10.1088/0951-7715/19/9/003, URL https://doi-org.bibliopass.unito.it/10.1088/0951-7715/19/9/003.

Calleja, R., García-Azpeitia, C., Lessard, J.P., Mireles, J.J.D., 2021. From the Lagrange polygon to the figure eight. I: Numerical evidence extending a conjecture of marchal. Celest. Mech. Dyn. Astron. 133 (2), 20, Article no. 10.

Chen, K., 2001. Action-minimizing orbits in the parallelogram four-body problem with equal masses. Ann. Math. 158 (4), 293–318.

Chenciner, A., Montgomery, R., 2000. A remarkable periodic solution of the three-body problem in the case of equal masses.. Ann. Math. 152 (2), 881–901.

Chenciner, A., Venturelli, A., 2000. Minima de L'intégrale D'action du Problème Newtoniende 4 Corps de Masses Égales Dans R3: Orbites 'Hip-Hop'. Celest. Mech. Dyn. Astron. 77 (2), 139–151.

Ciccarelli, R., Introna, M., Terracini, S., Vasile, M., 2025. New solutions for the symmetrical n-body problem through variational approach and optimisation techniques. Aerotec. Missili Spaz. doi:10.1007/s42496-025-00265-5.

Cravero, I., Introna, M., 2024. A study on optimisation methods in celestial mechanics.. Rend. Sem. Mat. Univ. Pol. Torino.

Di Ruzza, S., 2021. Classical and relativistic n-body problem: from levi-civita to the most advanced interplanetary missions. Eur. Phys. J. Plus 136 (11), 1136.

DipMathUniTO, 2024. SymOrb.jl. https://github.com/DipMathUniTO/SymOrb.jl.

dlfer, 2017. Symorb. https://github.com/dlfer/symorb.

Ferrario, D.L., 2024. Symmetries and periodic orbits for the n-body problem: about the computational approach. Preprint, arXiv:2405.07737 [math.CA].

Ferrario, D.L., Terracini, S., 2004. On the existence of collisionless equivariant minimizers for the classical n-body problem. Invent. Math. 155 (2), 305–362. doi:10.1007/s00222-003-0322-7, URL https://doi-org.bibliopass.unito.it/10.1007/s00222-003-0322-7.

Forman, R., 1998. Morse theory for cell complexes. Adv. Math. 134 (1), 90–145. doi:10.1006/aima.1997.1650.

Fukuda, H., Fujiwara, T., Ozaki, H., 2018. Morse index for figure-eight choreographies of the planar equal mass three-body problem. J. Phys. A 51 (14), 145201.

Fukuda, H., Fujiwara, T., Ozaki, H., 2019. Morse index and bifurcation for figure-eight choreographies of the equal mass three-body problem. J. Phys. A 52 (18), 185201. doi:10.1088/1751-8121/ab1270.

Fusco, G., Gronchi, G.F., Negrini, P., 2011. Platonic polyhedra, topological constraints and periodic solutions of the classical N-bodyproblem.. Invent. Math. 185, 283–332.

Galán-Vioque, J., Muñoz-Almaraz, F.J., Freire, E., 2005. Stability and bifurcation behavior of the figure eight solution of the three body problem. In: EQUADIFF 2003. World Scientific, EQUADIFF 2003. Proceedings of the international conference on differential equations, Hasselt, Belgium, July 22–26, 2003. Hackensack, NJ, pp. 464–469.

Guardia, M., Martín, P., Seara, T.M., 2016. Oscillatory motions for the restricted planar circular three body problem. Invent. Math. 203 (2), 417–492. doi:10.1007/s00222-015-0591-y, URL https://doi-org.bibliopass.unito.it/10.1007/s00222-015-0591-y.

Kapela, T., Simó, C., 2007. Computer assisted proofs for nonsymmetric planar choreographies and for stability of the eight. Nonlinearity.

Leigh, N.W.C., Stone, N.C., Geller, A.M., Shara, M.M., Muddu, H., Solano-Oropeza, D., Thomas, Y., 2016. The chaotic four-body problem in Newtonian gravity– I. identical point-particles. Mon. Not. R. Astron. Soc. 463 (3), 3311–3325. doi:10.1093/mnras/stw2178.

Llibre, J., Simó, C., 1980. Oscillatory solutions in the planar restricted three-body problem. Math. Ann. 248 (2), 153–184. doi:10.1007/BF01421955, URL https://doi-org.bibliopass.unito.it/10.1007/BF01421955.

Majer, P., Terracini, S., 1993a. Periodic solutions to some n-body type problems: the fixed energy case. Duke Math. J. 69 (3), 683–697. doi:10.1215/S0012-7094-93-06929-3, URL https://doi-org.bibliopass.unito.it/10.1215/S0012-7094-93-06929-3.

Majer, P., Terracini, S., 1993b. Periodic solutions to some problems of n-body type. Arch. Ration. Mech. Anal. 124 (4), 381–404. doi:10.1007/BF00375608, URL https://doi-org.bibliopass.unito.it/10.1007/BF00375608.

Majer, P., Terracini, S., 1995. On the existence of infinitely many periodic solutions to some problems of n-body type. Comm. Pure Appl. Math. 48 (4), 449–470. doi:10.1002/cpa.3160480404, URL https://doi-org.bibliopass.unito.it/10.1002/cpa.3160480404.

Mayer, G., 1933. Solutions voisines des solutions de Lagrange dans le problème des n corps. Ann. Obs. Bordx..

Montgomery, R., 2024. Four Open Questions for the N-Body Problem. Cambridge University Press, Cambridge, This book explores four major open questions in the N-body problem, using tools from algebraic geometry and KAM theory, and showcasing progress made over two decades..

Moore, C., 1993. Braids in classical dynamics. Phys. Rev. Lett. 70 (24), 3675–3679. doi:10.1103/PhysRevLett.70.3675, URL https://doi-org.bibliopass.unito.it/10.1103/PhysRevLett.70.3675.

Morse, M., 1934. The calculus of variations in the large. In: American Mathematical Society Colloquium Publications, vol. 18, American Mathematical Society, Providence, RI.

Moser, J., 1973. Stable and random motions in dynamical systems. In: Annals of Mathematics Studies, No. 77, Princeton University Press, Princeton, NJ; University of Tokyo Press, Tokyo, p. viii+198, With special emphasis on celestial mechanics, Hermann Weyl Lectures, the Institute for Advanced Study, Princeton, N. J.

Poincaré, H., 1893. Les Méthodes Nouvelles De La Mécanique Céleste, vol. 2, Gauthier-Villars et fils, imprimeurs-libraires.

Rabinowitz, P.H., 1978. Periodic solutions of Hamiltonian systems. In: Communications on Pure and Applied Mathematics, vol. 31, American Mathematical Society, pp. 157–184. doi:10.1002/cpa.3160310203.

Rackauckas, C., Nie, Q., 2017. Differentialequations.jl–a performant and feature-rich ecosystem for solving differential equations in julia. J. Open Res. Softw. 5 (1), 15.

Ramos, M., Terracini, S., 1995. Noncollision periodic solutions to some singular dynamical systems with very weak forces. J. Differential Equations 118 (1), 121–152.

Roberts, G.E., 2002. Linear stability of the elliptic Lagrangian triangle solutions in the three-body problem. J. Differential Equations 182, 191–218.

Roberts, G.E., 2007. Linear stability analysis of the figure-eight orbit in the three-body problem. Ergod. Theory Dyn. Syst. 27, 1947–1963.

Serra, E., Terracini, S., 1992. Collisionless periodic solutions to some three-body problems.. Arch. Ration. Mech. Anal. 120, 305–325.

Simó, C., 2001a. New Families of Solutions in N-Body Problems. Birkhäuser, 3rd European congress of mathematics (ECM), Barcelona, Spain, July 10–14, 2000. Basel.

Simó, C., 2001b. New families of solutions in N-body problems. In: Casacuberta, C., Miró-Roig, R.M., Verdera, J., Xambó-Descamps, S. (Eds.), European Congress of Mathematics. Birkhäuser Basel, Basel, pp. 101–115.

Simó, C., 2001c. Periodic orbits of the planar n -body problem with equal masses and all bodies on the SamePath.. IoP Publ. Bristol 265–284.

Smale, S., 1965. On the morse index theorem. J. Math. Mech. 14 (5), 1049–1055.

Teschl, G., 2012. Ordinary differential equations and dynamical systems, vol. 140, American Mathematical Society.

Vanderbei, R.J., 2004a. New orbits for the n-body problem. Ann. New York Acad. Sci. 1017, 422–433.

Vanderbei, R.J., 2004b. New orbits for the n-body problem. Ann. New York Acad. Sci. 1017 (1), 422–433.